LAWRENCE
LIVERMORE
NATIONAL
LABORATORY

LLNL-CONF-749900

A novel x-ray crystal spectrometer for the diagnosis of high energy density plasmas at the National Ignition Facilitya

M. Bitter, K. W. Hill, L. Gao, B. Kraus, P. C. Efthimion, M. B. Schneider, F. Coppari, R. Kauffman, A. MacPhee, Y. Ping, D. Thorn

April 19, 2018

High Temperature Plasma Diagnostics
San DIego, CA, United States
April 16, 2018 through April 19, 2018

Disclaimer

A novel x-ray crystal spectrometer for the diagnosis of high energy density plasmas at the National Ignition Facility[a)]

M. Bitter,[1,b)] K. W. Hill,[1] LanGao,[1] Kraus,[1] P. C. Eftihimion,[1] M. Schneider,[2] F. Coppari,[2] R. Kauffman,[2] A. McPhee,[2] Y. Ping,[2] and D. Thorn[2]

[1]*Princeton Plasma Physics Laboratory, Princeton, New Jersey 08543, USA*
[2]*Lawrence Livermore National Laboratory, Livermore, California 94550, USA*

(Presented XXXXX; received XXXXX; accepted XXXXX; published online XXXXX)
(Dates appearing here are provided by the Editorial Office)

The here-described spectrometer was developed for the Extended X-ray Absorption Fine Structure (EXAFS) spectroscopy of high-density plasmas at the National Ignition Facility (NIF), and it employs as the Bragg reflecting element at new type of toroidally bent crystal with a constant and very large major radius R and a much smaller, locally varying, minor radius r. The focusing properties of this crystal and the experimental arrangement of source and detector make it possible to **(a)** fulfill the conditions for a perfect imaging of an ideal point source for each wavelength, **(b)** obtain a high photon throughput, **(c)** obtain a high spectral resolution by eliminating the effects of source-size broadening, and **(d)** obtain a one-dimensional spatial resolution with a high magnification perpendicular to the main dispersion plane.

I. INTRODUCTION

According to F. Coppari et al. [1], 'X-ray diffraction (XRD) and the Extended X-ray Absorption Fine Structure (EXAFS) spectroscopy are among the most widely used diagnostics in high pressure condensed matter studies because of their capability to provide information about the structural transformations occurring in the material at the atomic level. And the EXAFS technique, in particular, is extremely powerful in discerning the local atomic environment.' - Reading this statement, one may be led to assume that the appropriate instrumentation for those EXAFS studies is readily available. But, it turns out that the simultaneous requirements of a high spectral resolution and a high photon-throughput, for an extended spectral range, cannot be met by any of the existing spectrometer types. Notably, the effects of source-size broadening, which limit the spectral resolution, have been so troubling that, ultimately, in order to mitigate these effects, painstaking 'source development' experiments were conducted at the NIF to reduce the source size itself [1].

An important step towards a solution of the source-size broadening problem by an improved spectrometer design was made by J. Koch [2], who proposed the use of a modified Johann spectrometer with a spherical Ge-220 crystal of a large radius of curvature **R** = 4826 mm, where the x-ray source would be close to the crystal to enhance the photon-throughput and where the detector would be placed on the Rowland circle to eliminate the effects of source-size broadening, since - for this position of the detector - the Johann aberration minimal and therefore negligible.

Koch's spectrometer design had, however, two shortcomings:

1. The distance, $d_{CS} = 150mm$, of the source from the central point on the crystal surface was much shorter than the crystal's sagittal focal length, which - for the main Bragg angle in Koch's design of $q_0 = 13.72°$ – amounted to $f_s = \frac{R}{2 \cdot \sin(q_0)} = 10174mm$. The image of the source was therefore a virtual image, which was located behind the crystal, at the distance, $d_{IM} = 152.24mm$, from the central point on the crystal's surface. The reflected rays, which seem to emanate from this virtual image, were therefore divergent, and their points of intersection with the detector plane were spread out on an elliptical arc of the length **H**, which was determined by the height **h** of the crystal:

$$H = \frac{d_{IM} + R \cdot \sin(q_0)}{d_{IM}} \cdot h = 8.5 \cdot h$$

so that for a modest height of the crystal of $h = 10mm$, the height of the detector needed to be $H = 85.2mm$ in order to collect all the reflected photons. The useful height of the crystal and hence the attainable photon throughput were thus ultimately limited by the height **H** of the detector. And the realization of Koch's idea of increasing the photon

[a)]Published as part of the Proceedings of the 22nd Topical Conference on High-Temperature Plasma Diagnostics (HTPD 2018) in San Diego, California, USA.
[b)]Author to whom correspondence should be addressed: bitter@pppl.gov

throughput by moving the source close to the crystal is thereby actually much constrained. – It is also not possible to increase the photon throughput beyond this limit by moving the source still closer to the crystal, since the reflected rays are then even more divergent.

2. Koch's other suggestion, namely, to eliminate the source-size broadening effects by placing the detector on the Rowland circle, is not specific enough and for his chosen orientation of the detector plane - perpendicular to the main reflected ray for the Bragg angle $q_0 = 13.72°$- the source-size broadening effects were eliminated only for the wavelength, associated with the Bragg angle q_0, rather than the entire spectral range.

Our new spectrometer design, which is described in section II, eliminates these shortcomings. It satisfies the conditions for perfect imaging for each wavelength and eliminates the effects of source-size broadening for the entire spectral range of interest, so that it is possible to obtain at once a high photon throughput, a high spectral resolution, and a high one-dimensional spatial resolution perpendicular to the main dispersion plane.

II. A NEW EXAFS SPECTROMETER

A. Spectrometer Design

The 'usual definition' of the Rowland circle – as a circle in the main dispersion plane, which passes through the center of curvature of the spherical crystal and the central point on the crystal surface and whose diameter is equal to the radius **R** of the crystal - is dissatisfying, since it breaks the rotational symmetry of the system without any reason by singling out this particular crystal point. In principle, one can construct an infinite number of equivalent circles with the diameter **R** that pass through the center of curvature of the spherical crystal and any crystal point in the main dispersion plane.

Instead of the Rowland circle, we therefore prefer to use the 'tangency' spheres with the radii $r = R \cdot \cos(q)$ about the center of the crystal sphere to which the incident and reflected rays with a Bragg angle Θ are tangential. The advantages of this different concept are that the spherical symmetry of the system is fully maintained and that all the crystal points are treated equally. In order to eliminate the source-size broadening effects for a certain Bragg angle Θ the detector must then be at the tangency point of the reflected ray with the sphere of the radius $r = R \cdot \cos(q)$, where the Johann aberration has a minimum.

In the following, we describe our design of an EXAFS spectrometer for the x-ray energies $8.877 £ E £ 10.877 keV$ which include the energy of the TaL3 absorption edge at 9.877 keV. The x-ray diffracting element is a toroidally bent Ge[400]-crystal with the 2d-lattice spacing of $2d = 2.82868 Å$ and the major radius $R = 3068 mm$. The distance of the source from the central point on the crystal surface is $d_{SC} = 280 mm$. The experimental arrangement is shown in Fig. 1.

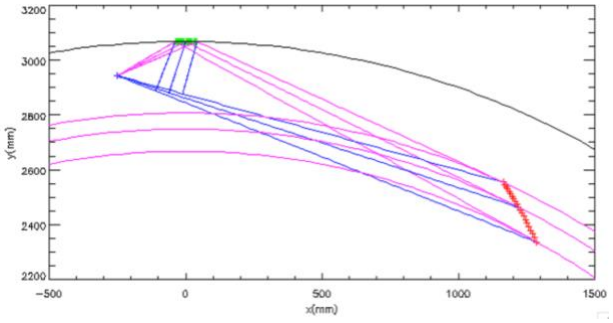

FIG. 1. Basic experimental arrangement of source, crystal and image points in the main dispersion plane, which was chosen as the x,y-plane of an x,y,z,-coordinate system.

The trace of the crystal in the main dispersion plane *(black curve)* is a circle with the radius **R** about the point x=0; y=0. The points, shown in green, represent 21 crystal points, which are the points of Bragg reflection for equidistant x-ray energies in the interval from 8.877 to 10.877 keV, and the points, shown in red, are the tangency points of the Bragg reflected rays with the circles of the radii $r = R \cdot \cos(q)$ about x=0, y=0 for the associated Bragg angles Θ. Only three of these tangency circles, for the energies E = 8.877; 9.877; 10.877 keV and the corresponding Bragg angles Θ = 29.588; 26.345; 24.482°, are shown in Fig. 1 together with the incident and reflected rays *(magenta color)*. Since the aforementioned tangency points are the points with the minimum Johann aberration, where source-size broadening effects are negligible, we establish these points as image points by demanding that the straight lines *(blue lines)*, which interconnect these tangency points with the source, are axes of rotational symmetry for the crystal. The short line segments *(blue)*, which are normal to these axes of rotational symmetry and extend from these axes up to the points of Bragg reflection, represent therefore the locally varying minor radii **r** of the toroidally bent crystal.

B. Dispersion

The wavelength dispersion is defined as $\frac{d\lambda}{ds}$, where λ and s are, respectively, the wavelength and the length of arc on which the image points are distributed in the detector plane. We use the following formulas:

$$(1) \qquad ds = \sqrt{1 + \left(\frac{dy_I}{dx_I}\right)^2} \cdot dx_I$$

where x_I and y_I are the coordinates of the image points in the detector plane.

Equation (1) can be rewritten as

$$(2) \qquad \frac{ds}{d\lambda} = \sqrt{1+\left(\frac{dy_I}{dx_I}\right)^2} \cdot \frac{dx_I}{d\lambda}$$

Figures 2 and 3 show the functions $y_i(x_I)$ and $x_i(\lambda)$ on a larger scale and demonstrate that these functions are well approximated by straight lines with the slopes $\frac{dy_I}{dx_I} = -1.787$ and $\frac{dx_I}{d\lambda} = 474.770\ [mm/\text{Å}]$. Inserting these numerical values in eq. (2), we get

$$(2') \qquad \frac{ds}{d\lambda} = 972.118\ [mm/\text{Å}]$$

and

$$(1') \qquad \frac{d\lambda}{ds} = 1.03\ [m\text{Å}/mm]$$

The required length of the detector to cover the energy range, 8.877 < E < 10.877 keV, is:

$$(3) \qquad s = \frac{ds}{d\lambda} \cdot (\lambda_1 - \lambda_2) = 249.7mm$$

where $\lambda_1 = 1.39669\text{Å}$ and $\lambda_2 = 1.13987\text{Å}$ are, respectively, the wavelengths which associated with the x-ray energies of 8.877 and 10,877 keV.

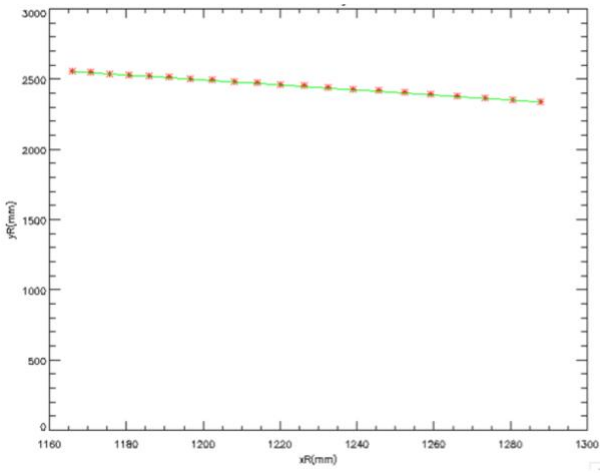

FIG. 2. Image points in the detector plane *(red)* and the straight line *(green)* connecting the end points (x_I=1165.93 mm, y_I=2554.36 mm) and (x_I=1287.86 mm, y_I=2336.51 mm).

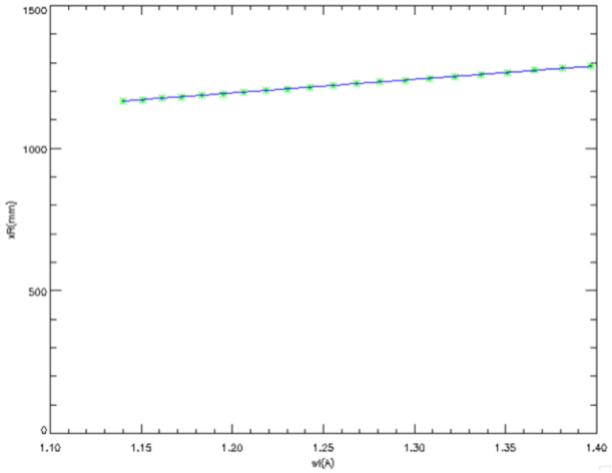

FIG. 3. Abscissa x_I of image points *(green)* as a function of λ and straight line *(blue)* connecting the endpoints.

III. DISCUSSION AND CONCLUSIONS

The novelty of our toroidal crystal spectrometer is a varying minor radius, which changes in magnitude and direction along the crystal surface to establish, at each crystal point, the proper rotational symmetry for the imaging of an ideal point source. The axis of the rotational symmetry for a set of crystal points, which represent the Bragg reflection points for a certain wavelength λ, is solely determined by the positions of the source point and image point for this particular λ, since the source and image points must be fixed points of a respective rotation and therefore lie on the axis. The image point is bound to the source point by the law of reflection and otherwise freely selectable. Therefore, one can, in particular, position the source close to the crystal to enhance the photon throughput and then select, for each wavelength, as image point the point with the minimum Johann aberration in order to eliminate the effects of source-size broadening. In doing so, one obtains not only a high spectral resolution but also a high spatial resolution with a large magnification perpendicular to the main dispersion plane. The here-described toroidal crystal spectrometer offers, therefore, a high degree of flexibility and new features, which are unmatched by any of the existing spectrometers. In fact, the type of toroidal crystal spectrometers, which are presently being used for the diagnosis of laser-produced plasmas – see, e.g. E. J. Gamoa et al. [3] - are distinctly different from here-described spectrometer due to the fact that these spectrometers use a conventional toroidal crystal form with a constant minor radius which at every crystal point is aligned with the normal to the crystal surface. With this geometry, it is possible to eliminate the source-size broadening effects and implement the conditions for perfect imaging for only one wavelength λ with the associated Bragg angle Θ(λ), if firstly the source and image are both at the same distance $R \cdot \sin[\alpha(\lambda)]$ from the point of Bragg reflection on the crystal surfaced and if secondly the minor radius r satisfies the relation

$r = R \cdot \sin^2[q(/)]$. One also obtains, for this particular wavelength, a spatial resolution perpendicular to the main dispersion plane with a magnification of one. For all other wavelengths and all other source and detector positions, the basic physics principles for imaging are violated.

We plan to use our new toroidal crystal spectrometer design for EXAFS studies of the TaL3 absorption edge at the Laboratory for Laser Energetics (LLE) in Rochester in the fall of 2018.

IV. ACKNOWLEDGEMENTS

This work was performed under the auspices of the U. S. DoE by LLNL under Contract DE-AC52-07NA27344 and PPPL under contract DE-AC02-09CH11466.

[1]F. Coppari, D. B. Thorn, G. E. Kemp, R. S. Craxton, E. M. Garcia, Y. Ping, J. H. Eggert, and M. B. Schneider, Rev. Sci. Instrum. **88**, 083907 (2017).
[2]J. Koch, LLNL X-ray Spectroscopy Workshop 2015.
[3]E. J. Gamboa, C. M. Huntington, M. R. Trantham, P. A. Keiter, R. P. Drake, D. S. Montgomery, J. F. Benage, and S. A. Letzring, Rev. Sci. Instrum. **83**, 10E108 (2012).